Geotech Geol Eng (2013) 31:199–212
DOI 10.1007/s10706-012-9580-8

ORIGINAL PAPER

Investigating the Effects of Local Contact Loss on the Earth Pressure Distribution on Rigid Pipes

Sherif Kamel · Mohamed A. Meguid

Received: 3 March 2011 / Accepted: 20 October 2012 / Published online: 30 October 2012

Abstract In this paper, the earth pressure distribution acting on a buried pipe with localized support loss is investigated experimentally and numerically in this study. A laboratory setup has been designed to facilitate the simulation of the local wall separation and to track the changes in earth pressure at selected locations along the pipe circumference. Validated by the experimental results, two-dimensional finite element analysis has been conducted to examine the role of soil-pipe interaction on the pressure distribution around the pipe before and after the contact loss is introduced. Experimental and numerical results revealed that the presence of a gap between the pipe wall and the surrounding backfill can lead to significant changes in contact pressure and bending moment in the pipe wall in the immediate vicinity of the gap. This study suggests that efforts to detect and repair areas experiencing support loss should be made before significant changes in pressure develop causing stress concentration in the pipe wall as it may lead to pipe damage.

S. Kamel · M. A. Meguid (✉)
Civil Engineering and Applied Mechanics, McGill University, 817 Sherbrooke Street West, Montreal, QC H3A 2K6, Canada
e-mail: mohamed.meguid@mcgill.ca

S. Kamel
e-mail: sherif.kamel@mail.mcgill.ca

Keywords Rigid pipes · Earth pressure distribution · Contact loss · Subsurface soil erosion · Finite element · Physical models

1 Introduction

Buried pipes are essential infrastructure, as they supply the society with indispensable services (e.g. sanitary and drainage networks, watermains and natural gas pipelines). Different methods are available to calculate the earth pressure transferred to buried pipes, including empirical (Marston and Anderson 1913; Spangler and Handy 1973); analytical (Burns and Richard 1964; Hoeg 1968) and numerical analyses (Katona and Smith 1976; Tohda et al. 1990). The soil condition around pipes is of prime importance for the structural performance of these structures. Full contact is usually assumed between the pipe and the surrounding backfill throughout the service life of the pipe.

After construction, different factors can negatively affect the performance of buried pipes, including disintegration of structural parts, chemical attack, and soil erosion (Jewell 1945). A thorough description of the structural deterioration of rigid pipes has been reported by Davies et al. (2001). Selected studies that have recently evaluated the effect of contact loss and void formation around buried structures are reviewed in the following sections.

Tan and Moore (2007) investigated numerically the effect of void formation on the performance of buried rigid pipes. The influence of both the void size and location (e.g. springline and invert) on the stresses and bending moments in the pipe wall was investigated. Results of an elastic model showed that the presence of a void at springline leads to an increase in the extreme fiber stresses and bending moments at all critical locations: crown, springlines and invert. The rate of increase is controlled by the growth of the void in contact with the rigid pipe. Extending the model to include the soil shear failure resulted in stresses and moments higher than those reported in the elastic analysis. Changing the location of the void from springline to invert resulted in reduction in bending moment values followed by a reverse of the moment sign.

Meguid and Dang (2009) studied numerically the effect of erosion void formation around an existing tunnel on the circumferential stresses in the lining. A series of elastic–plastic finite element analyses was carried out to investigate the effect of different parameters (e.g., flexibility ratio, coefficient of earth pressure at rest and void size) on thrust forces and bending moments in the lining. When the void was located at the springline, bending moment significantly increased. Similar results were reported for the thrust forces under the same conditions regardless of the flexibility ratio. The presence of erosion void at the lining invert was found to reduce the bending moments causing reversal in the sign of the moment as the void size increased.

Leung and Meguid (2011) conducted an experimental investigation to measure the changes in earth pressure around a tunnel lining due to the introduction of a local contact loss at different locations around the lining. The results showed that earth pressure increased locally around the separated section with a maximum increase of 25 % at the springline. The above studies illustrate the significant changes in earth pressure and internal forces in the walls of a buried structure when the soil separates locally from the structures.

Talesnick and Baker (1999) reported the failure of a large diameter (1.2 m) concrete-lined steel sewage pipe buried in clayey soil. Field investigations revealed the formation of a physical gap of approximately 20 mm between the invert and the bedding layer supporting the pipe. Severe cracking developed at the crown and springline along a 300 m segment of the pipeline. This case study emphasizes the importance of a full contact between the buried structure and the supporting soil.

The objective of this study is to investigate the changes in earth pressure resulting from a local contact loss induced at different locations between the backfill and the wall of an existing pipe. A schematic showing a local support loss at the invert of a rigid pipe is shown in Fig. 1 along with a simplified physical model. A series of laboratory experiments is conducted to evaluate the effect of local separation between the pipe wall and the surrounding soil on the earth pressure distribution acting on the pipe and the measured results are compared with the initial earth pressures. Three different locations of local contact loss are examined in this experimental study namely; springline, haunch, and invert (see Fig. 2).

Elasto-plastic finite element analyses are then performed to examine the role of soil-pipe interaction in the redistribution of earth pressure around the pipe and bending moment in the pipe wall. The numerical model is first validated by simulating the actual experiment and comparing the calculated pressures with those measured in the laboratory. The model is then used to assess the applicability of the experimental technique used to simulate the soil void around the pipe. Conclusions are made regarding the pressure increase resulting from the created void as compared to initial conditions.

2 Experimental Setup

A series of experiments was conducted to examine the changes in earth pressure acting on a buried pipe subjected to local contact loss. A description of the

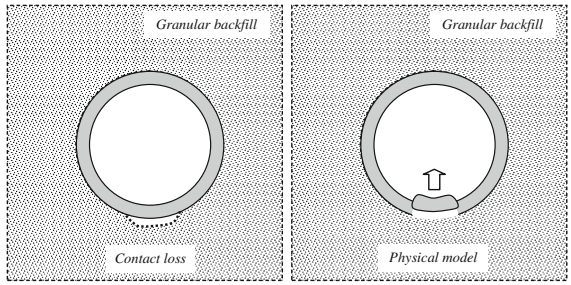

Fig. 1 Rigid pipe subjected to local contact loss

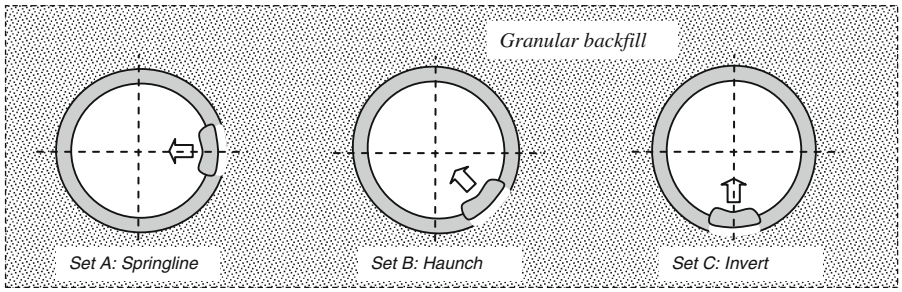

Fig. 2 The three test sets investigated experimentally

different components and the procedure of the experiment is given below.

2.1 Steel Tank

The testing facility has been designed such that the entire pipe model was contained in a rigid steel tank. As illustrated in Fig. 3, the tank is approximately 1,410 mm long, 1,270 mm high and 300 mm wide with a 12 mm plexiglass face. Both the front and rear sides were reinforced using three 100 mm HSS sections. The internal steel sides of the tank were painted and lined with plastic sheets to reduce friction between the sand and the sides of the tank. On the front and rear sides, a hole of 152 mm in diameter was drilled. The hole size was selected to be larger than the outer diameter of the pipe to ensure that the pipe rests directly on the sand. The location of the opening was chosen to minimize the influence of the rigid boundaries on the measured earth pressure and to ensure sufficient overburden pressure over the pipe (C/D = 2). This was achieved by placing the lateral boundaries at a distance approximately four times the pipe diameter (4.2 D) measured from its circumference. The rigid base of the tank was located at a distance of 2.2 D below the pipe invert.

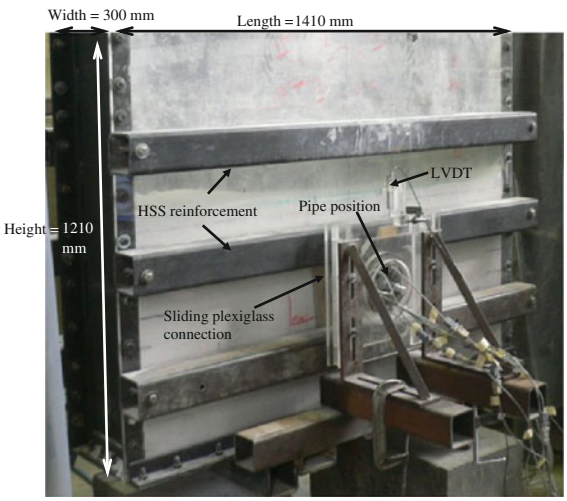

Fig. 3 Experimental setup

2.2 Steel Pipe

One of the challenges of the experimental setup was to develop a suitable mechanism to simulate the local contact loss between the pipe wall and the surrounding medium while recording the earth pressure changes around the pipe. This was achieved by designing and machining a segmented pipe composed of six curved segments sliced from a cold drawn steel pipe of 25 mm wall thickness (114 mm in diameter, and 610 mm in length) and six aluminum strips. To hold the different circular sectors of the pipe, six stainless steel U-shape grooved pieces were used and reinforcing stiffeners were used to ensure the pipe rigidity (see Fig. 4a). The different pipe sectors were assembled such that the segments tightly fit between the lips of the holding pieces. The U-shaped pieces were hinged to a 25 mm hexagonal nut screwed to a threaded rod passing along the pipe length. The movement of the nuts allows for a total shrinkage of the outer diameter of the pipe by 3 mm. The aluminum shims were placed such that one end is bolted to one of the pipe segments while the other end is left to slide freely over the adjacent segment. The small gaps between the shim and the pipe were sealed with clear silicon caulking so that sand particles do not enter between the segments and damage the sensors. The different parts used in assembling the segmented pipe are shown in Fig. 4a, whereas the fully installed pipe is shown in Fig. 4b. Under full expansion condition, the pipe outer diameter is 150 mm.

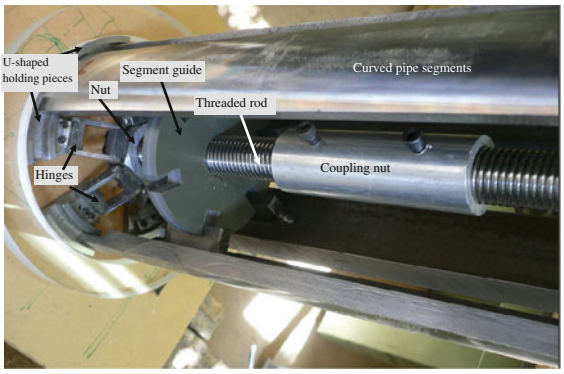

(a)

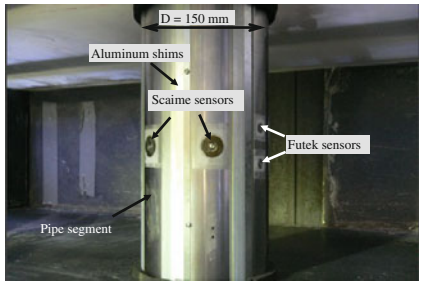

(b)

Fig. 4 The segmented pipe **a** different parts used in assembling the segmented pipe and **b** assembled pipe spanning the steel tank

To simulate the local contact loss between the pipe wall and the backfill material, a slot of 10 mm wide and 260 mm long was opened along the length of one of the pipe segments. This opening served to host a steel strip, of similar dimension and geometry, machined from another tube of the same curvature. The movement of the steel strip was controlled using hinges and two threaded rods connected at the centre of the pipe segment by a custom made coupling nut. To move the steel strip, a threaded rod was turned, causing the hinges to move towards the coupling nut and therefore the steel strip moves inward. The strip movement was calibrated to retract exactly 1.5 mm per full 360° rotation with a maximum retraction of 3.5 mm. The pipe was designed so that the retractable strip could be placed at the springline, haunch and invert. The dimensions of the retractable steel strip would correspond to approximately 1.5 % of the pipe circumference or a void angle of 5.1° as compared to Meguid and Dang (2009) and Tan and Moore (2007), respectively. Figure 5a, b show the inside and outside views of the retractable strip, respectively.

2.3 Instrumentation

To measure the earth pressure distribution, the pipe was instrumented with eight load cells connected to a data acquisition system. Four of them (Scaime AR) have maximum capacity of 1,200 g with accuracy of ±0.02 % while the remaining ones (Futek LBB) have maximum capacity of 250 g with accuracy of ±0.05 %. All load cells were mounted inside the pipe with only the sensing area installed flush with the pipe

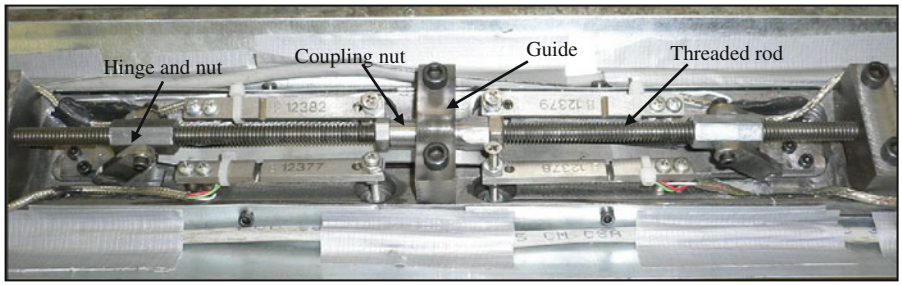

(a)

(b)

Fig. 5 The retractable strip **a** inner mechanism and **b** outer side

circumference and exposed to the soil. The diameter of the sensing area was 25 and 12 mm for the Scaime and Futek sensors, respectively. Scaime sensors were installed along a circular cross section at the middle of the pipe. Futek sensors were placed on both sides of the retractable strip and ±19 mm from the middle of the pipe (see Fig. 4b). Such arrangement of the sensors allowed the changes in earth pressure to be monitored in the close vicinity of the strip and at other critical locations along the pipe circumference. It should be emphasized that the sizes of the different load cells were selected such that all sensors fit inside the pipe (particularly the four sensors around the retractable strip) and at the same time provide the accuracy needed for the expected changes in soil pressure. The locations of the load cells were chosen based on the previously conducted numerical study (Meguid and Dang 2009) which concluded that changes in earth pressure develop mainly in the close vicinity of the void. A schematic showing the position and numbering of the sensors is shown in Fig. 6.

2.4 Fine Sand

Quartz sand was used as the backfill material. Sieve analysis, direct shear and other soil property tests were performed on several randomly selected samples. The density of the sand in the tank was also measured during the tests by placing small containers of known volume at different depths inside the tank. The coefficients of uniformity (C_u) and curvature (C_c) of the sand were found to be 1.90 and 0.89, respectively.

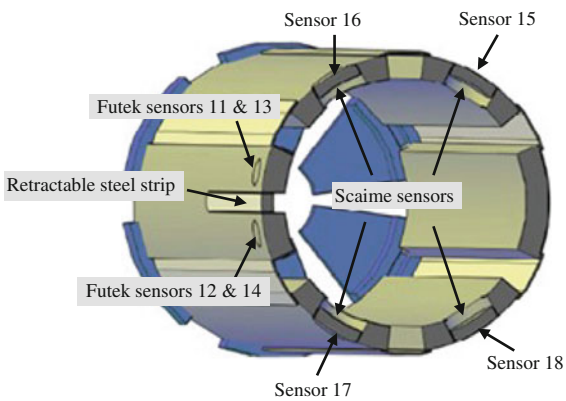

Fig. 6 A schematic showing half the pipe and all sensor locations

Table 1 Soil properties

Property	Value
Specific gravity	2.66
Coefficient of uniformity (C_u)	1.9
Coefficient of curvature (C_c)	0.89
Maximum dry unit weight (γ_{max})	15.7 kN/m^3
Minimum dry unit weight (γ_{min})	14.1 kN/m^3
Experimental dry unit weight (γ_d)	15.0 kN/m^3
Unified soil classification system	SP
Internal friction angle (ϕ)	38.5°
Cohesion (c)	0.2 kPa
Coefficient of earth pressure at rest (K_o)	0.38

A summary of the sand properties is provided in Table 1.

3 Testing Plan

3.1 Load Cell Calibration

To ensure that the load cells measure the correct pressure, the entire pipe model was subjected to a hydrostatic pressure and the readings were recorded and compared to the expected pressure values. At a depth of 0.9 m below water surface, the maximum hydrostatic pressure was measured to be 8.6 kPa which is in agreement with the theoretical value expected of $\gamma_w h_w = 9.81 \times 0.9 = 8.8$ kPa. The load cells were also mounted on the side of a rigid vertical wall (0.5 m in height and 1 m in length) and subjected to lateral soil pressure induced by sand backfill. Results indicated a linearly increasing pressure with depth. The load cells readings were consistent with the expected at-rest earth pressure under two-dimensional condition ($\gamma h K_0$). The coefficient of lateral earth pressure at rest, K_o, was calculated using ($1 - \sin\phi = 0.38$). The angle of internal friction, ϕ, was obtained from direct shear tests performed on the sand used throughout the entire experimental program.

3.2 Procedure

The procedure consisted of installing the pipe under contracted condition (144 mm OD) in the tank. As the pipe crosses the tank face, two rubber membranes having 150 mm diameter hole were slipped from

inside the tank along the pipe. The pipe was expanded to its maximum diameter (150 mm) and its horizontal position was checked. While monitoring the horizontal position of the pipe, two machined plexiglass connections were installed at the extremities of the pipe to facilitate free sliding in the vertical direction (see Fig. 3). The external plexiglass connections attached to the pipe were lifted and clamped to prevent the pipe from resting directly on the rigid boundaries of the tank and allowing for the placement of the soil under the pipe invert while the pipe is at a temporary elevated position. The role of the rubber membranes was to prevent the sand leakage that may occur from the existing gap between the pipe and the tank. To monitor the horizontal position of the pipe while the test is running, two vertical LVDTs were attached to the plexiglass connections and connected to the data acquisition system.

After securing the pipe in its temporary position, a testing procedure was developed in order to ensure consistent initial conditions (i.e. sand density) throughout the conducted experiments. The sand was rained from a constant height into the tank in layers. From the tank base up to the pipe invert, the soil was placed in three layers 100 mm in height. Each layer was first graded to level the surface then tamped using a steel plate attached to a wooden handle. The sand placement continued up to the pipe invert. Above the invert, the rained sand was gently pushed around the pipe up to the crown to ensure full contact between the sand and the pipe. At this stage, the sensors were switched on to record the earth pressure applied. Then, another layer of sand was added to cover completely the pipe. The remaining sand required to reach the height of 2D above the crown was placed with no tamping to minimize damage to the load cells. The clamps holding the pipe were then removed simultaneously allowing the pipe to slide vertically and rest on the bedding sand layer. The horizontal position of the pipe was checked through the recorded readings of the vertical LVDTs attached to the plexiglass connections.

Once the initial conditions were established, the next step was to retract the steel strip to simulate a local support loss between the pipe and the backfill soil. Since the strip could retract up to 3 mm, the retraction was split into two steps each representing a movement of 1.5 mm away from the sand. After each step, the sensor readings were recorded and the test completed. Finally, after the test, while the tank was being emptied, the sand sampling cups were recovered and the sand density was measured.

3.3 Tests Performed

Three sets of tests were conducted following the described procedure above to examine the effect of the retracted strip location (springline, haunch and invert) on the changes in earth pressure acting on the pipe as shown in Fig. 2. The sequence of the sensors varied for each set of tests according to the position of the retracted section. Three tests were performed for each position of the retracted section with a total of nine tests conducted in this study.

4 Experimental Results

The earth pressure results presented in this section are based on the load cell readings taken at the sensor locations along the pipe circumference. The results of the nine tests conducted (three tests for each position) revealed consistent changes in earth pressure readings recorded by the load cells located in the close vicinity of the retractable strip. In all tests, the readings of the sensors located away from the retractable section did not register significant changes in pressure after introducing the local contact loss. Figure 7 shows the changes in contact pressure recorded by sensors 15 through 18, when the retracted section was positioned at the springline. The measured earth pressure, p, is normalized with respect to the initial pressure, p_0, and plotted on the vertical axis whereas the retractable section movement, Δ (mm), is plotted on the horizontal axis. Insignificant changes in earth pressure were measured at the above locations with a maximum pressure increase of 4 % as recorded by sensor 16 for a retraction of 3 mm. This behavior is consistent with the findings of Meguid and Dang (2009), who concluded that changes in lining response occur mostly in the close vicinity of the introduced void.

Earth pressure changes in the vicinity of the retracted section are presented in Figs. 8 through 10. The pressure readings when the gap was introduced at the springline, haunch, and invert are discussed in the following sections. In addition, a summary of the percentage change in earth pressure measured in the three sets of tests is presented in Table 2.

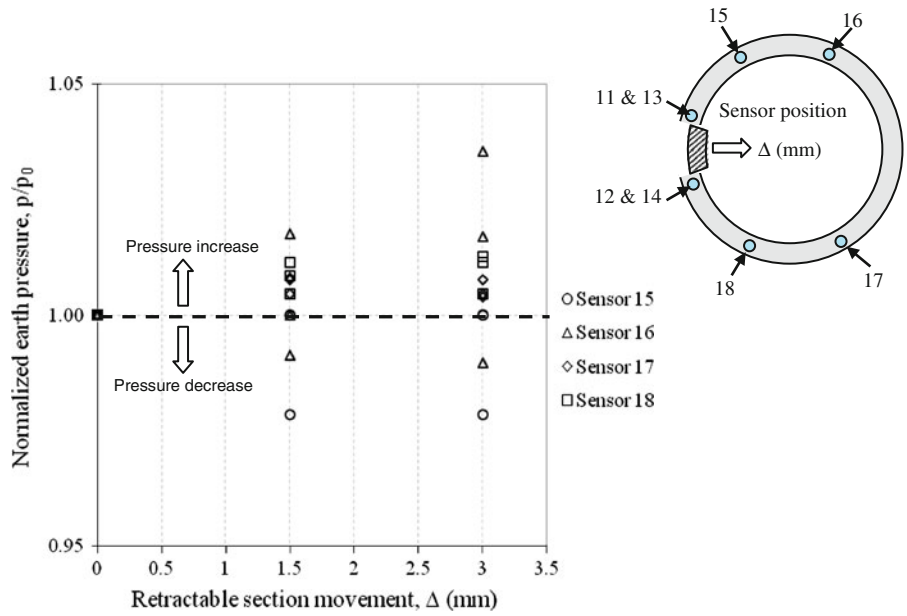

Fig. 7 Measured changes in earth pressure away from the retracted strip—at the springline

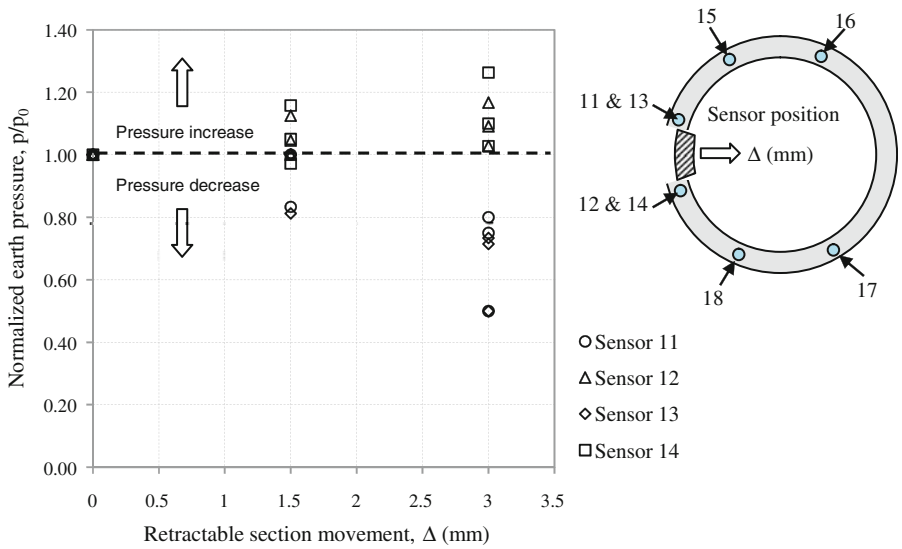

Fig. 8 Measured changes in earth pressure around the retracted strip—at the springline

4.1 Contact Loss at the Springline

Figure 8 presents the changes in contact pressure measured by the load cells located in the vicinity of the retractable section, for a local contact loss at the springline. Different pressure readings were registered by the sensors located above and below the retractable section. Sensors 11 and 13 located above the retractable section recorded gradual reduction in pressure, while sensors 12 and 14 located below the section registered gradual increase in pressure. For a retraction of 1.5 mm, the upper sensors recorded a maximum pressure reduction of 20 %. This pressure reduction was accompanied by a pressure increase of 18 % as recorded by the lower sensors. This behavior can be explained by the observed soil movement behind the strip under gravity filling the created void and causing additional pressure around the lower sensors. Further retraction of the section to 3 mm, the pressure registered by the upper sensors dropped to 50 % of

Table 2 Summary of the measured changes in pressure at the sensor locations around the pipe

	% Change in pressure at sensors 11 and 13						% Change in pressure at sensors 12 and 14					
	Test 1		Test 2		Test 3		Test 1		Test 2		Test 3	
Set A: Springline												
Retraction of 1.5 mm	−17	−19	0	0	0	0	+5	+5	+13	+16	0	−3
Retraction of 3 mm	−50	−50	−20	−29	−25	−27	+9	+10	+17	+26	+3	+3
Set B: Haunch												
Retraction of 1.5 mm	+3	+3	+2	+2	0	+3	0	+7	0	+5	+4	0
Retraction of 3 mm	+10	+8	+7	+8	+10	+13	+15	+21	+9	+16	+17	+17
Set C: Invert												
Retraction of 1.5 mm	+13	+6	N/A[a]	+7	0	0	+8	+6	+11	+13	0	0
Retraction of 3 mm	+17	+11	N/A[a]	+15	+17	+18	+13	+10	+22	+19	+15	+15

[a] In this test the sensors malfunctioned due to sand clogging

the initial pressure, whereas, the lower sensors recorded 30 % increase in pressure.

4.2 Contact Loss at the Haunch

Figure 9 shows the changes in contact pressure measured by the sensors located in the vicinity of the retractable section when located at the haunch. Sensors on both sides registered an increase in contact pressure induced by the progressive retraction of 1.5 and 3 mm. For a retraction of 1.5 mm, the pressure increased by 7 % of the initial value and continued to increase to about 21 % of the initial pressure when the retraction reached 3 mm.

4.3 Contact Loss at the Invert

Moving the position of the retractable section to the invert resulted in similar behavior to that reported at the haunch where sensors on both sides registered pressure increase (see Fig. 10). For a 1.5 mm retraction, the pressure increased by 12 % of the initial value and further increased to 22 % when the movement of the retractable section reached 3 mm.

To visualize the relative changes in contact pressure, the average of the measured pressure changes registered by the sensors (11/13 and 12/14) located at the boundaries of the retractable section are presented in Fig. 11a, b based on the nine conducted tests. For a retraction of 3 mm, the changes in pressure were

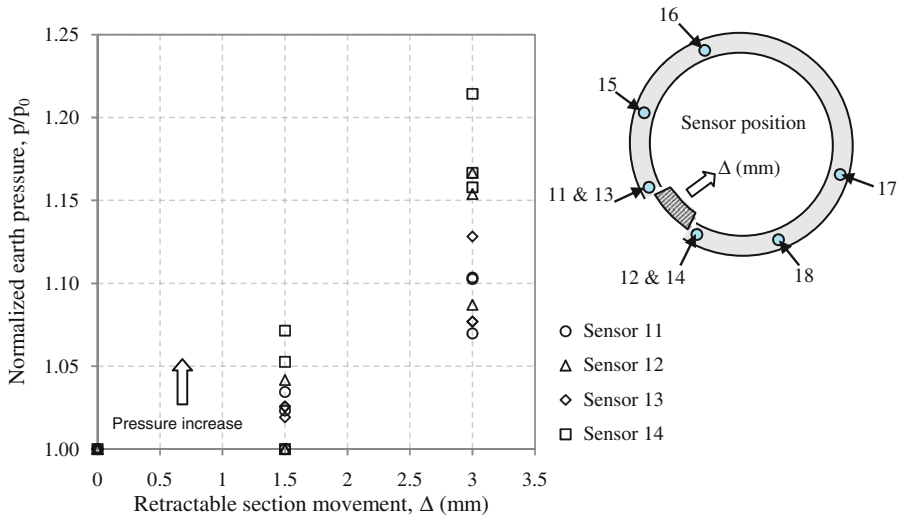

Fig. 9 Measured changes in earth pressure around the retracted strip—at the haunch

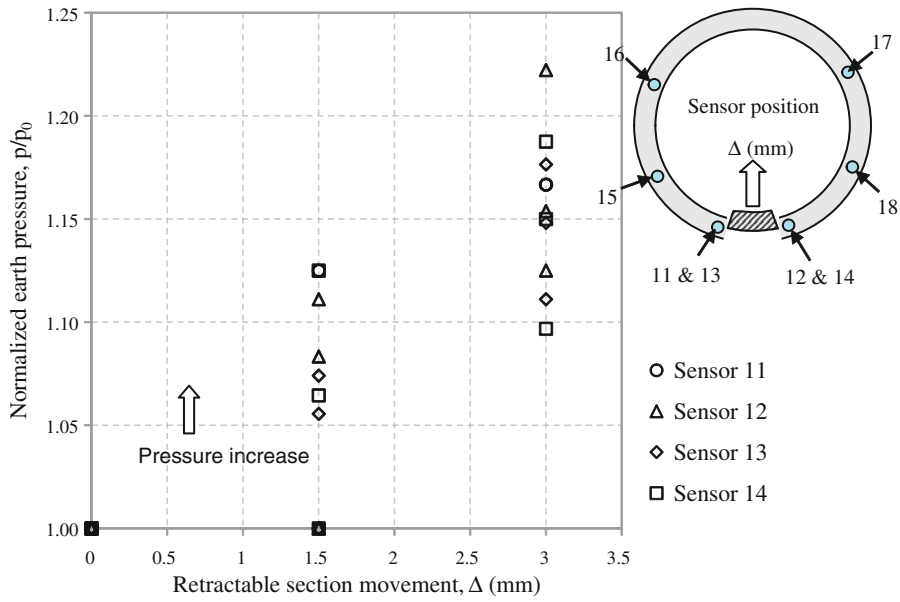

Fig. 10 Measured changes in earth pressure around the retracted strip—at the invert

generally greater compared to those recorded for 1.5 mm retraction. This behavior confirms that, for the investigated length of the wall separation, the earth pressure significantly changes in the vicinity of the area that has experienced contact loss.

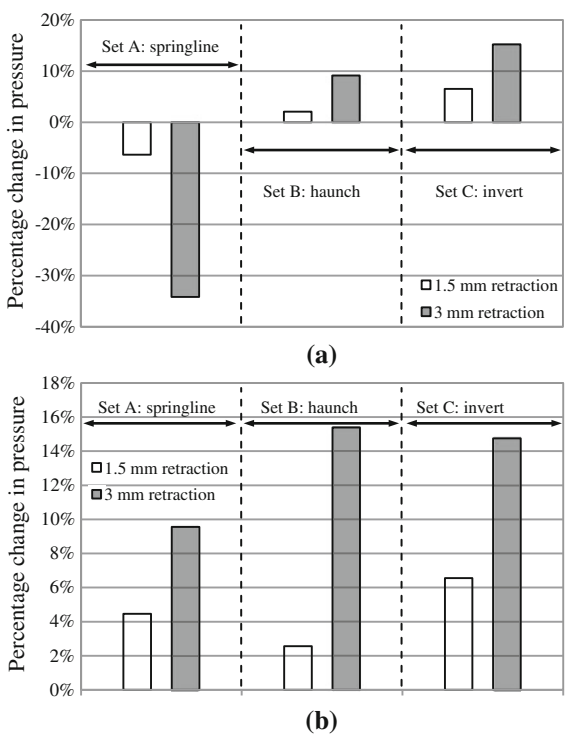

Fig. 11 Average changes in pressure as recorded by **a** sensors 11 and 13 and **b** sensors 12 and 14

5 Numerical Analysis

Finite element analyses have been conducted to simulate the experimental set up and investigate the role of soil-pipe interaction on the changes in earth pressure resulting from the introduction of a local contact loss between the backfill soil and the pipe wall.

The analyses were performed using ABAQUS version 6.9 finite element program. The soil was modeled using Mohr–Coulomb failure criterion with the following parameters: density = 1.5 t/m^3; friction angle = 38.5°; dilation angle = 27°; elastic modulus = 10 MPa; Poisson's ratio = 0.3; coefficient of earth pressure at rest = 0.38. The pipe was modeled as linear elastic material with the following parameters: Density = 7.8 t/m^3; Elastic modulus = 200 GPa; Poisson's ratio = 0.3. The soil density used in the numerical analysis is consistent with that measured during the experiments as described in Sect. 2.4. The soil friction angle is obtained from direct shear tests performed on selected sand samples. The deformation parameters, on the other hand, were chosen in consistency with the values recommended by McGrath et al. (1999) using the available soil properties (grain size, relative density and stress level).

The boundary conditions were selected to represent smooth rigid side boundaries and a rough rigid base boundary. Both the soil and the pipe were modeled using continuum elements (C2D8 8-noded quadratic) throughout the analysis. A typical finite element mesh for the condition of a contact loss at the springline is shown in Fig. 12. The interaction between the soil and the buried pipe is modeled using the surface-to-surface interaction technique. Both fully bonded and free slippage interface conditions between the soil and the pipe were simulated. It is worth noting that the free slippage interface condition was modeled by defining normal and tangential contact properties with friction coefficient of 0.01.

The stage construction and sand placement procedure used in the experiments was duplicated in the numerical analysis. The steps used were as follow:

1. Generating the in situ geostatic stresses in the base soil layer. The coefficient of earth pressure was taken as $K_o = 1 - \sin\phi$ (ϕ = angle of internal friction of the soil).
2. The pipe and the first soil layer (around the pipe) are activated.
3. The soil layer above the pipe crown is activated.
4. The final soil layer is activated to reach the target level.

To simulate the local retraction of the steel strip, the mesh of the pipe wall was discretized with element sizes that correspond to the displacements used in the experiments. Using the element deactivation and activation procedure allowed for the sequential retraction to be simulated.

6 Model Validation and Numerical Results

Figure 13 shows the initial earth pressures calculated along with the experimentally measured values before the gap introduction. Higher pressures were generally calculated at the invert compared to the crown and springline. It was found that, at the sensor locations, the numerical model was able to reasonably capture the pressure distribution around the pipe. The interface condition was found to affect the calculated pressures at the crown (90°) and invert (270°) as illustrated by the solid and broken lines in Fig. 13. However, since the change in earth pressure due to local contact loss is of prime interest in this study and the initial conditions are generally used as a reference, the results of the numerical analysis are considered acceptable.

A numerical investigation was conducted to evaluate the effect of the section retraction technique used in the experiments on the measured earth pressures. The void was simulated numerically by incrementally removing the eroded soil elements from the model leaving a gap between the pipe and the surrounding soil. The results are then compared to the experimental data and presented in the polar plot as illustrated in Fig. 14. The difference between the measured and calculated pressures at the sensor locations was found to be insignificant. In addition,

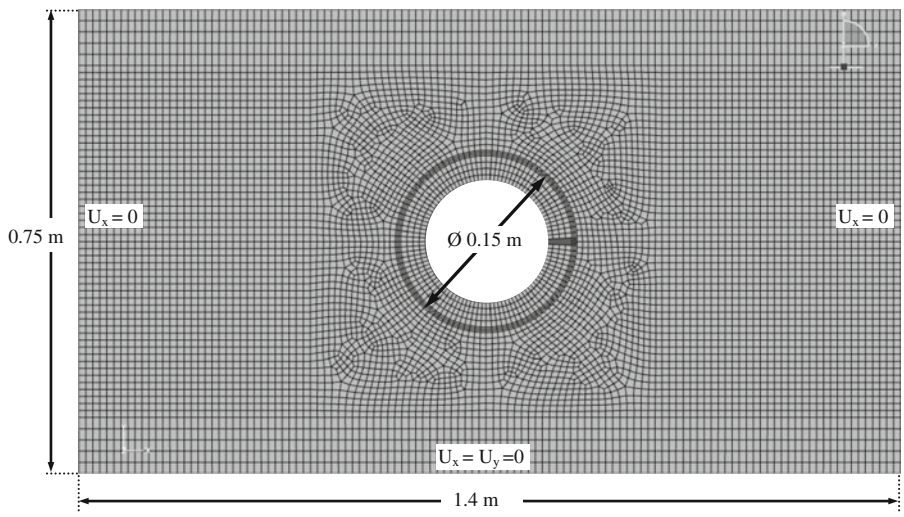

Fig. 12 Typical finite element mesh

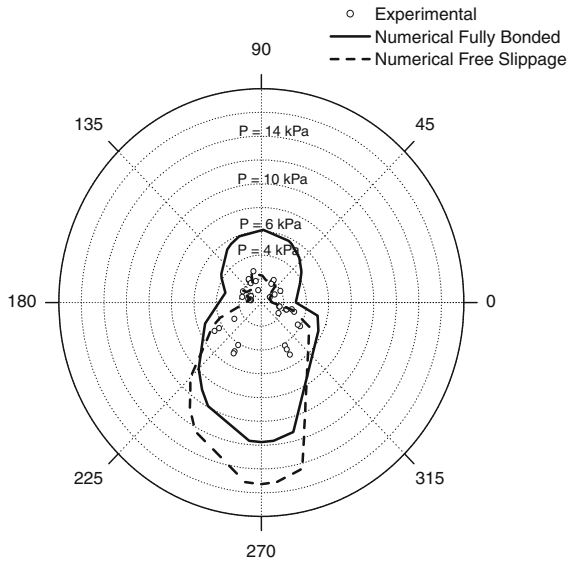

Fig. 13 Measured and calculated initial earth pressure (in kPa) before void introduction

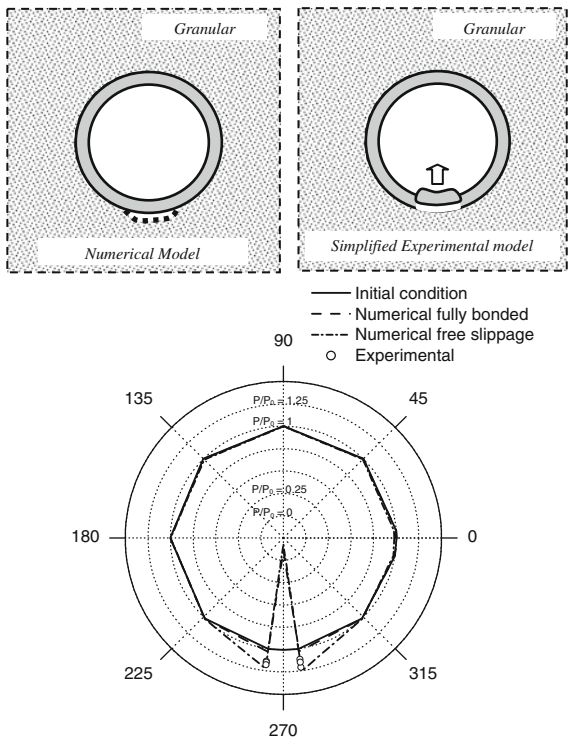

Fig. 14 Changes in earth pressure due to contact loss introduced at the invert evaluating the effect of the simplified experimental physical model

the measured pressures were found to be located between the two investigated interface conditions. These results indicate that the retracted section approach used in the experiments had little effect on the measured earth pressure.

The role of interface condition is further investigated in Fig. 15 using polar plots of the measured and calculated changes in pressure using free slippage and fully bonded interface between the pipe and the surrounding soil. It was found that the numerically calculated changes in pressure are independent of the retracted distance (1.5 and 3 mm). This is attributed to the continuum nature of the model that does not allow particle movement and, therefore, the only final state of stresses for 3 mm retraction is used in this section. The earth pressure, p, is normalized with respect to the initial pressure, p_0, and plotted on the radial directions for different angles with the horizontal. At the springline Fig. 15a, a mix of pressure increase and decrease was calculated at the boundaries of the induced gap; the reduction in pressure is found to be about 50 % and the increase in pressure is about 25 %. At the haunch and invert (Fig. 15b, c), a consistent pressure increase of 20 % at the gap boundaries is calculated. The results calculated represented the upper and lower bounds of the contact pressure. Based on the results presented in Fig. 15, it has been noted that the measured pressures are bound by those numerically calculated under fully bonded and free slippage interface conditions with more tendency towards the fully bonded interface. This can be explained by the fact that the actual interface between the pipe and the soil is not perfectly smooth particularly around the retracted section due to the presence of the sensors.

Figure 16 presents the regions of the soil yield (represented by maximum difference in principal stresses) when the voids were introduced at the springline, haunch and invert, respectively. It can be noticed that, for the investigated gap size, soil failure is generally located around the gap boundaries where most of the stress concentration is measured.

Finally, pipe stresses has been calculated numerically for the pipe geometry and material properties used in the experiment. However, the presence of the additional transverse reinforcement inside the pipe resulted in stress levels that are considered insignificant.

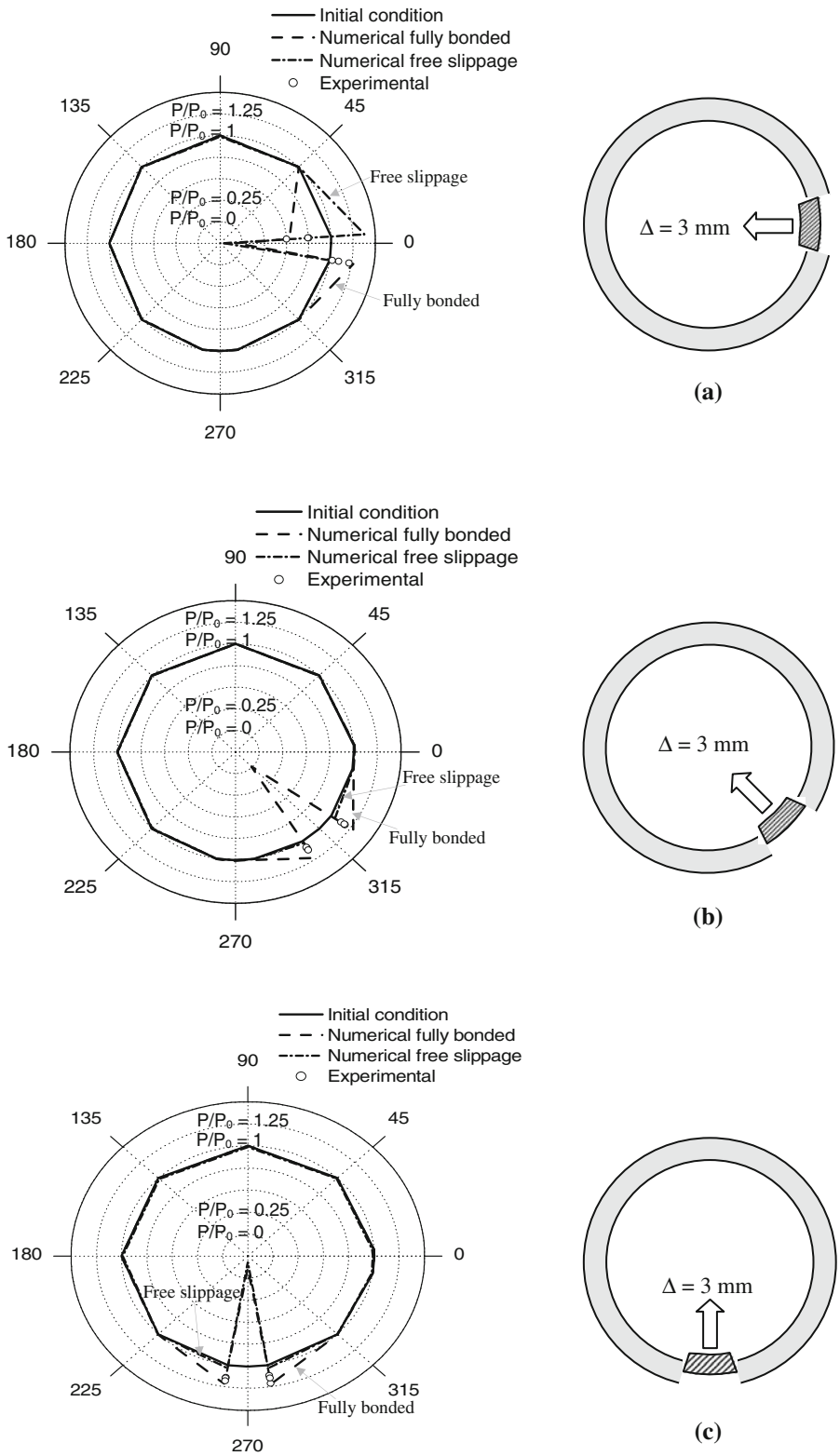

Fig. 15 Comparison between the calculated and measured earth pressures at the **a** springline, **b** haunch, and **c** invert

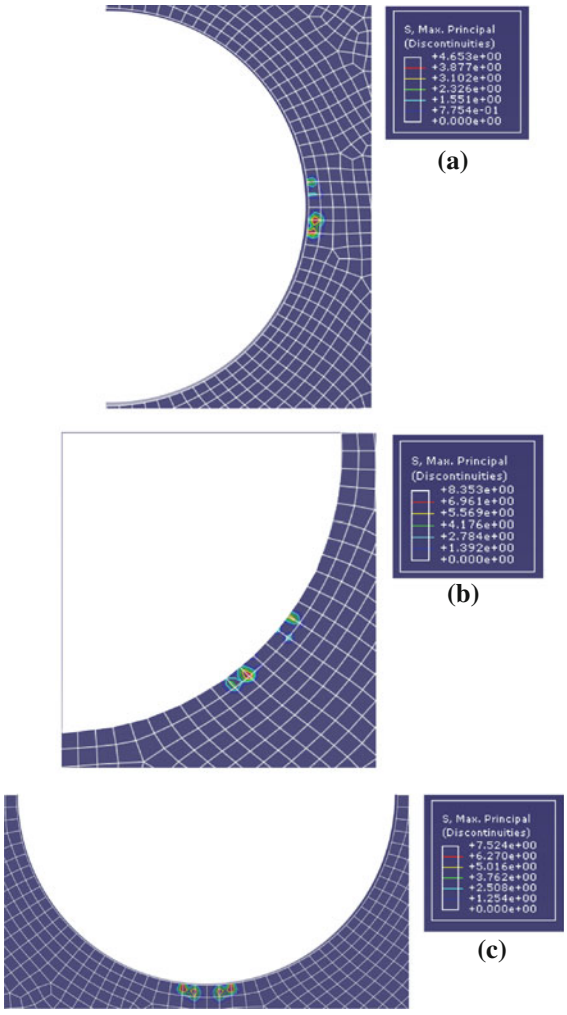

Fig. 16 Soil yield regions around the pipe for a gap at **a** springline, **b** haunch and **c** invert

7 Changes in Pipe Moments

As the pipe stresses and moments were not measured directly in the experiments, the validated finite element model has been used to study the impact of void size on the bending moment developing in the pipe walls. Four different void sizes were used in the analysis representing void angles of 5°, 10°, 20° and 40°. These voids were introduced next to the pipe wall at the springline and invert and the corresponding changes in moment at (a) springline, (b) invert and (c) crown are evaluated. A shown in Fig. 17, when the void was located at the springline, the increase in void size has results in moment increase that was maximum at the springline (about 30 %) and decreased to about

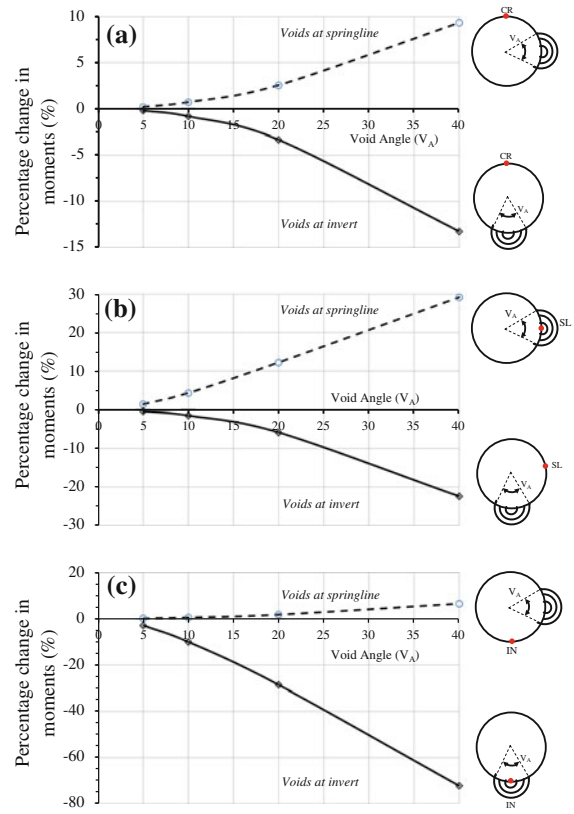

Fig. 17 Changes in pipe moments **a** crown, **b** springline and **c** invert

10 % towards the crown and invert. On the other hand, when the void was located at the invert, the moment increased by about 70 % at the invert and decreased to about 15 % towards the crown.

8 Summary and Conclusions

Experimental and numerical investigations have been performed to examine the effect of contact loss between a steel pipe and the surrounding soil on the changes in earth pressure distribution acting on the pipe. A mechanically retractable strip 10 mm in width and 260 mm in length positioned at three different locations (springline, haunch and invert) has been used to simulate the contact loss. The load cells installed at the boundaries of the retractable section measured the changes in earth pressure. The progressive movement of the retractable section from 1.5 to 3 mm caused additional changes in pressure around the area experiencing the contact loss. Based on the nine tests conducted in this study and the two-dimensional

numerical simulations performed, the following conclusions were reached:

1. In granular soils, a void may develop along the lower half of the pipe circumference. The void size and location are considered to be the main controlling parameters affecting the earth pressure distribution around the pipe.
2. The introduction of a local contact loss at the springline caused pressure increase of about 30 % of the initial value immediately below the separation zone and a decrease of about 50 % above.
3. At the haunch and invert, the introduction of local contact loss caused a consistent increase in earth pressure at the boundaries of the gap with a maximum increase of 22 % of the initial pressure.

Elasto-plastic finite element analyses have been performed to investigate the effect of soil-pipe interaction on the earth pressure distribution around the created gap at the springline and invert. The earth pressure calculated using the finite element method confirmed that most of the changes in pressure take place at the close vicinity of the gap. The changes in pressure measured in the experiments were located between those calculated numerically for fully bonded soil-pipe interface and free slippage conditions. Bending moments were also calculated numerically and were found to increase as the void size increased. The maximum change in moment in the pipe wall was found near the void location for the case where the void was placed at the invert.

The results presented in this study have an interesting practical significance related to the impact of contact loss that may develop between an existing steel pipe and the surrounding soil. As the gap develops, pressures acting on the pipe may increase or decrease depending on the void location with respect to the pipe circumference. The increase in pressure means that the pipe structure may be subjected to stresses that were not considered in the design. While the decrease of pressure seems of less significance, it is equally critical as the reduction of stresses at a certain location is usually associated with an increase of stresses elsewhere causing rapid change of stresses within a limited area. Although, pipe damage was not directly measured in this study, it is expected that as the void size increases, the increase in moment may lead to stress concentration and possible cracking of the pipe structure.

It should be noted that this study has examined the earth pressure distribution acting on a model steel pipe buried in granular medium, and is considered a starting point for engineering investigation of these issues. Full scale tests of actual rigid pipes and three-dimensional models are needed to verify the above findings.

Acknowledgments This research is supported by the Natural Sciences and Engineering Research Council of Canada (NSERC) under grant number 311971-06. The assistance of Mr. John Bartczak in building the experimental setup is appreciated.

References

Burns JQ, Richard RM (1964) Attenuation of stresses for buried cylinders. In: Proceedings, symposium of soil–structure Interaction, Arizona University, pp 378–392

Davies JP, Clarke BA, Whiter JT, Cunningham RJ (2001) Factors influencing the structural deterioration and collapse of rigid sewer pipes. Urban Water 3(1–2):73–89

Hoeg K (1968) Stresses against underground structural cylinders. American Society of Civil Engineers Proceedings, Journal of the Soil Mechanics and Foundation Division, 94(SM4), pp 833–858

Jewell HW (1945) Factors affecting service life of underground pipe structures. Brick Clay Rec 106(1):39–42

Katona MG, Smith JM (1976) Modern approach for structural design of culverts. IPC Science and Technology Press, Ltd, Guildford, Surrey, pp 128–140

Leung C, Meguid MA (2011) An experimental study of the effect of local contact loss on the earth pressure distribution on existing tunnel linings. Tunn Undergr Space Technol 26(1):139–145

Marston A, Anderson AO (1913) The theory of loads on pipes in ditches and tests of cement and clay drain tile and sewer pipe. Iowa State College of Agriculture, Ames, p 181

McGrath T, Selig ET, Webb MC, Zoladz GV (1999) Pipe interaction with backfill envelop, US Department of Transportation, Federal Highway Administration. Publication No. FHWA-RD-98-191

Meguid MA, Dang HK (2009) The effect of erosion voids on existing tunnel linings. Tunn Undergr Space Technol 24(3):278–286

Spangler MG, Handy RL (1973) Soil engineering. Intext Educational, New York

Talesnick M, Baker R (1999) Investigation of the failure of a concrete-lined steel pipe. Geotech Geol Eng 17(2):99–121

Tan Z, Moore ID (2007) Effect of backfill erosion on moments in buried rigid pipes. Transportation Research Board Annual Conference, Washington, DC

Tohda J, Mikasa M, Hachiya M, Nakahashi S (1990) FE elastic analysis of measured earth pressure on buried rigid pipes in centrifuge models. In: Pipeline Design and Installation: Proceedings of the international conference, Las Vegas, NV, USA, pp 557–571